Pump controlled flexible generation between dissipative soliton and noise-like pulse from a mode-locked Er-doped fiber laser

XI CHENG,[1] QIANQIAN HUANG,[1] CHUANHANG ZOU,[1] CHENGBO MOU,[1,*] ZHIJUN YAN,[2] KAIMING ZHOU,[3] AND LIN ZHANG[3]

[1]Key Laboratory of Specialty Fiber Optics and Optical Access Networks, Shanghai Institute for Advanced Communication and Data Science, Joint International Research Laboratory of Specialty Fiber Optics and Advanced Communication, Shanghai University, Shanghai 200444, China
[2]School of Optical and Electronic Information, National Engineering Laboratory for Next Generation Internet Access System, Huazhong University of Science and Technology, Wuhan 430074, China
[3]Aston Institute of Photonic Technologies (AIPT), Aston University, Aston Triangle, Birmingham, B4 7ET, UK
**Corresponding author: mouc1@shu.edu.cn*

Received XX Month XXXX; revised XX Month, XXXX; accepted XX Month XXXX; posted XX Month XXXX (Doc. ID XXXXX); published XX Month XXXX

We experimentally investigate the alternative generation of dissipative solitons (DSs) or noise-like pulses (NLPs) from a passively mode-locked Er-doped all-fiber laser with 45° tilted fiber grating (45° TFG). The 45° TFG serves as an in-fiber polarizer for mode locking in the all-fiber laser cavity. Under the fixed orientations of the polarization controllers, flexible generation between DSs and NLPs can be precisely controlled by adjusting the pump power only. To the best of our knowledge, the total cavity length 4.92 m of our fiber laser is the shortest one among all of NLP fiber laser. We obtain the DS with 3 dB bandwidth of 20.4 nm centered at 1577 nm and the NLP with 3 dB bandwidth of 25.2 nm centered at 1574 nm. The fundamental repetition rate of the mode-locked pulses is 42.3 MHz. This DS-NLP switchable Er-doped fiber laser can be regarded as a multi-functional optical source for diverse practical and potential applications.

http://dx.doi.org/10.1364/AO.99.099999

1. INTRODUCTION

Passively mode-locked fiber lasers (PMLFLs) have aroused great attention due to their potential in achieving ultrafast light sources in recent decades [1-3]. So far, versatile operating regimes of PMLFLs have been demonstrated such as the conventional soliton (CS) regime [4], the dispersion-managed soliton (DMS) regime [5], the similariton regime [6] and the dissipative soliton (DS) regime [7]. It is well known that DSs can be generated from all-normal dispersion fiber lasers or large net normal dispersion fiber lasers. DS has much higher energy compared with CS and DMS because the pulse accumulates large chirp when it propagates in a normal dispersion cavity [8-10]. The DS with strongly chirped feature can also be easily amplified and compressed [11]. Therefore, DS fiber lasers with high quality output pulse can regarded as economic and compact seed light sources for high-power applications, such as micromachining and laser surgery. A representative characteristic of DS is that the spectrum has steep edges [12].

In addition to operating in the aboved-mentioned regimes which are expected to produce stable and coherent ultrashort pulses, PMLFLs can also operate in the so-called noise-like pulse (NLP) regime [13-16]. NLP has aroused intense research interests due to the characteristics of high energy, wide spectrum and low-coherence since it was reported by Horowitz *et al* for the first time in 1997 [17]. The NLP fiber laser has wide applications in the fields of optical sensors [18], supercontinuum generation [19,20] and optical coherence tomography [21]. In general, NLP has a nanosecond envelope and the interior of the envelope consists of a series of sub-picosecond secondary-pulses with random variations in terms of both intensity and width [17].

To date, several investigations of switchable generation between DS and NLP in the normal fiber laser have been reported [22-26]. However, it is hard to realize these two output pulse types with precise control in most fiber lasers. In fact, in some practical applications, the demands of the operation regime of fiber laser are very strict. So it is highly meaningful to improve the controllability of this DS-NLP switchable regime fiber lasers and to further explore whether DS and NLP can be switched to one another by only changing one parameter with other conditions fixed.

In this paper, we experimentally investigate the alternative generation of DSs and NLPs from an all fiber net normal dispersion laser by employing a 45° tilted fiber grating (45° TFG) as an intracavity polarizer. The most distinctive feature of our fiber laser is that the output pulse types can be precisely controlled by adjusting the pump power. The obtained DSs have an optical spectrum with the steep edges with the 3dB bandwidth of 20.4 nm centered at 1577 nm, and typical generated NLPs have a wide optical spectrum with the 3dB bandwidth of 25.2 nm centered at 1574 nm. A relatively short cavity length corresponds to 42.3 MHz fundamental repetition rate. The demonstrated laser features the highest fundamental repetition rate NLP generation by far. This DS-NLP switchable fiber laser with precise pump power control can be considered as multi-functional optical source for non-linear optical frequency transformation [27] and investigation of nonlinear dynamics [24,28]. Even more, to the best of our knowledge, this is the first time to generate NLPs from an Er-doped fiber laser (EDFL) based on a 45° TFG.

2. FABRICATION AND CHARACTERISTICS OF THE FIBER POLARIZING GRATING

A 244 nm frequency-doubled argon ion laser works as an ultraviolet laser source for grating inscription on a single mode fiber 28 (Corning SMF28e) by a phase mask technique to obtain 45° TFG in the experiment. The description of 45° TFG fabrication process is detailed elsewhere [29]. Both polarization dependent loss (PDL) and insertion loss spectrum of the 45° TFG are measured by an optical vector analyzer (LUNA system) with 1pm spectral resolution covering the spectral range from 1525 nm to 1608 nm.

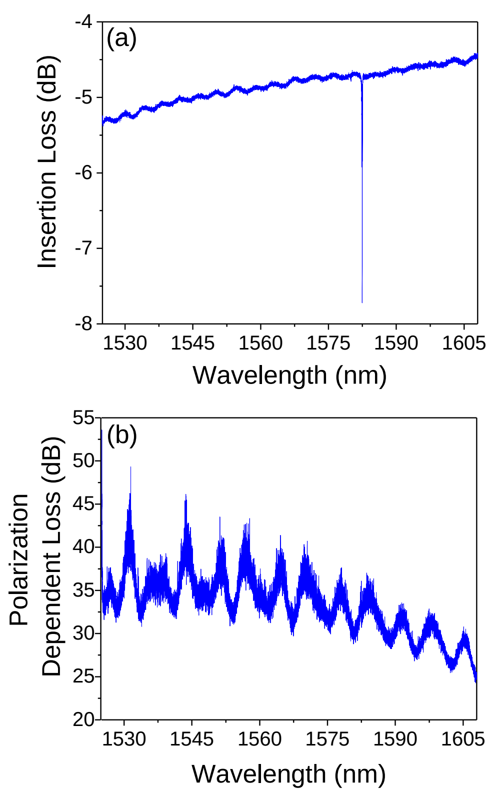

Fig. 1. Measured (a) insertion loss, and (b) PDL spectrum of the 45° TFG from 1525 to 1608 nm.

45° TFG is a type of special fiber grating with designated polarization dependent characteristics, which is able to tap out the *s*-light and propagate the *p*-light. Therefore, it can work as an ideal in-fiber polarizer by transforming the non-polarized light to linearly polarized light [30,31]. Compared with some standard bulk polarizers, 45° TFG benefits from the strong polarization dependent loss (PDL), low insertion loss and compact structure [31]. The typical insertion loss spectrum of the 45° TFG is depicted in Fig. 1(a). It can be clearly seen that the insertion loss of 45° TFG at 1575 nm is about 4.6 dB. The measured insertion loss is mostly composed of a huge transmission loss of *s*-light and extra loss due to bad splicing and connection, which manifests the low insertion loss of *p*-light [29]. There is an obvious narrow dip in the insertion loss spectrum around 1583 nm, which mainly caused by the second-order stimulated Bragg resonance [32]. In the light of the previous report [32], it can be known that the narrow dip has no significant effect on the performances of the grating. The PDL of the 45° TFG is shown in Fig. 1(b). Obviously, the value of PDL is wavelength dependent, and the maximum PDL value at 1575 nm is ~33 dB, the minimum PDL at 1608 nm is ~25dB, which means the 45° TFG is an excellent wideband in-fiber polarizer. So compared with some standard bulk polarizers, 45° TFG possesses the advantages of strong PDL, low insertion loss and all-fiber structure [31]. The ripples existing in insertion loss and PDL spectrum are both caused by the refractive index (RI) mismatching between the cladding and air [29]. Such ripples also can be removed by immersing the grating in the RI matching gel.

3. EXPERIMENTAL SETUP

The experimental schematic diagram of our proposed fiber laser is depicted in Fig. 2. The laser cavity is comprised of 148 cm highly doped EDF (OFS EDF80) with the group velocity dispersion (GVD) of +60.1 ps^2/km, 90 cm OFS 980 fiber with the GVD of +4.5 ps^2/km, and 243 cm single mode fiber (SMF) with the GVD of -22.8 ps^2/km. The overall cavity length is about 4.92 m, matching well the measured fundamental repetition rate. To the best of knowledge, this is the shortest cavity length of the NLP fiber laser. Therefore, our fiber laser is more compact, robust and controllable, which indicates it owns various advantages. Furthermore, the net dispersion of whole cavity is estimated to be +0.046 ps^2, which can support to generate DS.

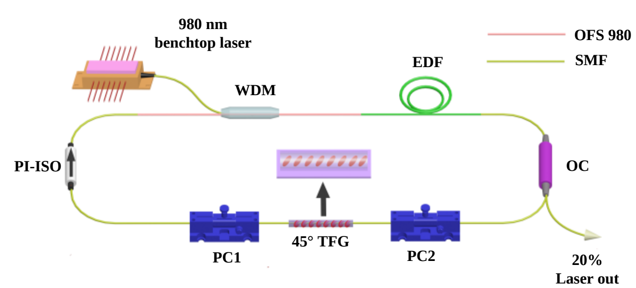

Fig. 2. Schematic setup of a net normal dispersion Er-doped fiber laser using a 45° TFG.

A 980 nm benchtop laser with 673 mW maximum pump power is used for pumping the EDF. The wavelength division multiplexer (WDM) is applied for coupling the 980 nm laser to the EDFL cavity, which is placed before the EDF. The 20:80 optical coupler (OC) taps out 20% cavity laser power. The polarization state of the cavity is adjusted by two polarization controllers (PCs) (PC1 and PC2). The 45° TFG is placed between two PCs to realize nonlinear polarization rotation (NPR) mechanism for mode locking. A polarization-independent isolator (PI-ISO) is utilized to enforce the single direction operation of the cavity. An optical spectrum analyzer (OSA, Yokogawa AQ6370C), a commercial autocorrelator, a 8 GHz high speed oscilloscope together with a 12.5 GHz fast photodetector, and a radio-frequency (RF) spectrum analyzer are applied for recording the laser output.

4. EXPERIMENTAL RESULTS AND DISCUSSIONS

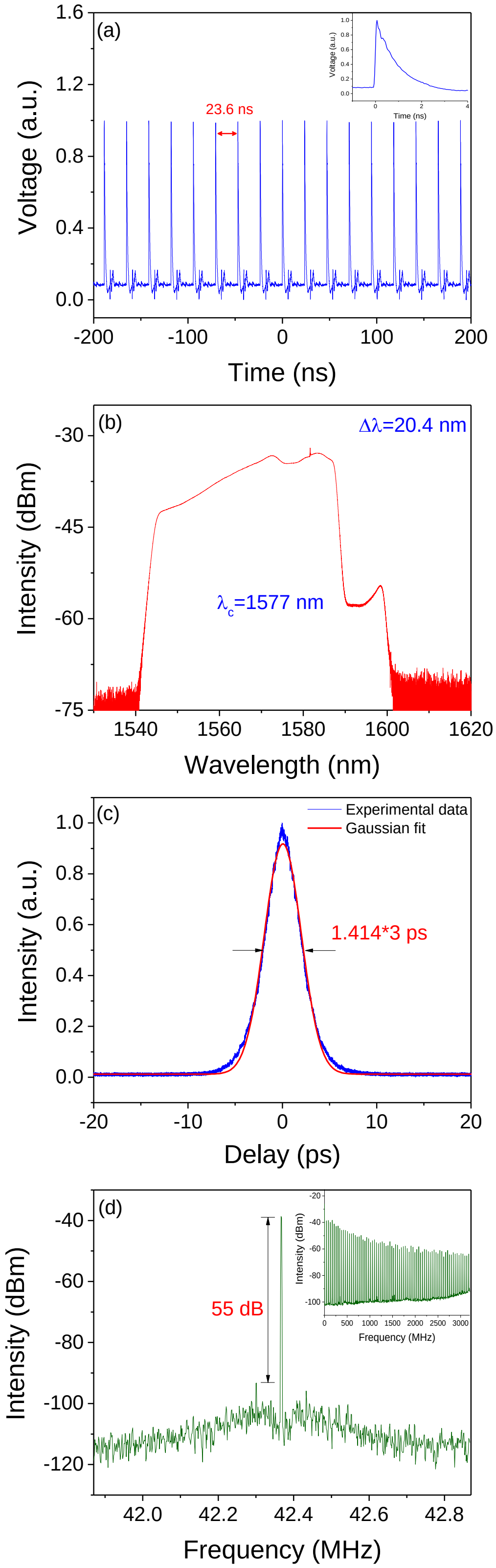

Fig. 3. Output characteristics of the DSs at pump power of 300 mW, (a) pulse train. Inset: single pulse, (b) optical spectrum, (c) AC trace, and (d) RF spectrum with a 1 MHz span and 1 kHz resolution bandwidth. Inset: RF spectrum with a 3.2 GHz span and 10 kHz resolution bandwidth.

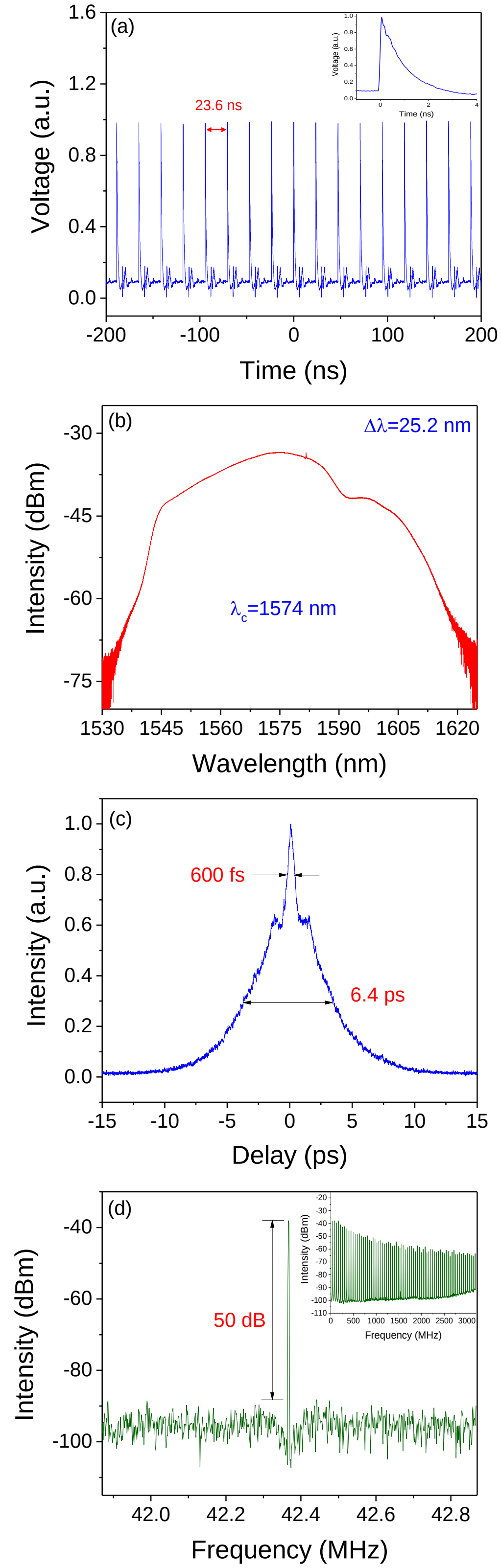

Fig. 4. Output characteristics of the NLPs at pump power of 300 mW, (a) pulse train. Inset: single pulse, (b) optical spectrum, (c) AC trace, and (d) RF spectrum with a 1 MHz span and 1 kHz resolution bandwidth. Inset: RF spectrum with a 3.2 GHz span and 10 kHz resolution bandwidth.

In our laser, when the pump power is set at 300 mW, the output pulse states switch between DS and NLP with the different PCs setting. It is well known that NPR not only acts as an equivalent saturable absorber (SA), but also can form a birefringent filter in the fiber laser [33]. Adjusting the PCs changes the cavity birefringence, which is equivalent to changing the spectral transmission in the cavity [34]. Therefore, the bandwidth of the artificial cavity birefringence filter can be adjusted by the PCs [34]. As the filtering effect is one of the conditions for promoting the formation of DS, we can obtain the DS mode locking at proper orientations of PCs. The performances of the DSs under 300 mW pump power is shown in Fig. 3. The pulse temporal sequence of the DSs is presented in Fig. 3(a). The time interval of the adjacent pulses is 23.6 ns, matching the fundamental repetition rate. The inset shows the single shot pulse of the DS regime. The measured optical spectrum of the DSs centering at 1577 nm with a 3 dB bandwidth of 20.4 nm is shown in Fig. 3(b). The optical spectrum with steep rising and falling edges is the indication of the DS operation. There is a clear sideband in the spectrum at 1598 nm, which maybe mainly caused by modulation instability [35]. It can also be seen a narrow small spike in the spectrum around 1583 nm, owing to the insertion loss spectrum with the narrow dip at 1583 nm illustrated in Fig. 1(a) [36]. We further measure the AC trace of the DSs, which is represented in Fig. 3(c). The recorded pulse duration is 3 ps when assumed the Gaussian pulse profile. Therefore, the calculated time-bandwidth product (TBP) is 7.4, signifying that the pulse is highly chirped. The RF represented signal-to-noise ratio (SNR) of 55 dB as shown in Fig. 3(d), which indicates that the operation of DS is relatively stable.

It is commonly known that NPR as an artificial SA allows the high intensity part of the pulse to pass with high transmission, while the low intensity part of the pulse wings suffers high loss. The extremum of the NPR transfer function was defined as the critical saturation power (CSP) [25]. Once the peak power exceeds the CSP, the effective cavity feedback mechanisms transformed from one to another [25]. This feedback conversion mechanism is the main reason for the formation of NLP in the fiber laser using NPR technique [14,16,25]. Actually, the adjustment of the PCs can result in the change of the CSP in a NPR mode locked fiber laser [25]. Under the standard scenario, we can easily observe that the pulse shaping regime transformation from DS to NLP by adjusting the PCs carefully under the fixed pump power of 300 mW. Fig. 4 reveals the characteristics of the NLP generated in such case. The oscilloscope pulse trace is depicted in Fig. 4(a), indicating the time interval of the adjacent pulses is 23.6 ns. The inset shows the single shot pulse of the NLP regime. The broad and smooth optical spectrum without steep edges is presented in Fig. 4(b). The center wavelength is turned to 1574 nm and 3 dB bandwidth is changed to 25.2 nm, which is wider than that of DSs. The AC trace with double-scale structure clearly shows a narrow spike on a wide pedestal in Fig. 4(c), which is the remarkable feature of NLP [17]. The FWHM of the spike and the pedestal are 620 fs and 6.4 ps, respectively. Fig. 4(d) is the RF spectrum of the NLPs, and the SNR is about 50 dB. There are two symmetrical sidelobs on the RF spectrum, indicating the inherent instability of the internal structure [37-39]. Besides, both of the output pulse types can work stably for several hours without spontaneously switching to another pulse state.

One distinct feature of our laser is that, when the DSs is obtained under 300 mW pump power, with just the pump power slowly increasing to 313 mW, the output pulse states can be changed from DSs to NLPs. This NLPs operation could be kept by increasing the pump power to 326 mW. Further pump power elevation makes the NLP operation unstable and finally disappear [24]. But if we lower the pump power to around 326 mW without changing any other conditions in our fiber laser, the NLP mode locking state can obtain again, and further reducing the pump power can switch the operation states from NLP to DS. It is worth noting that this process is repeatable and reversible,

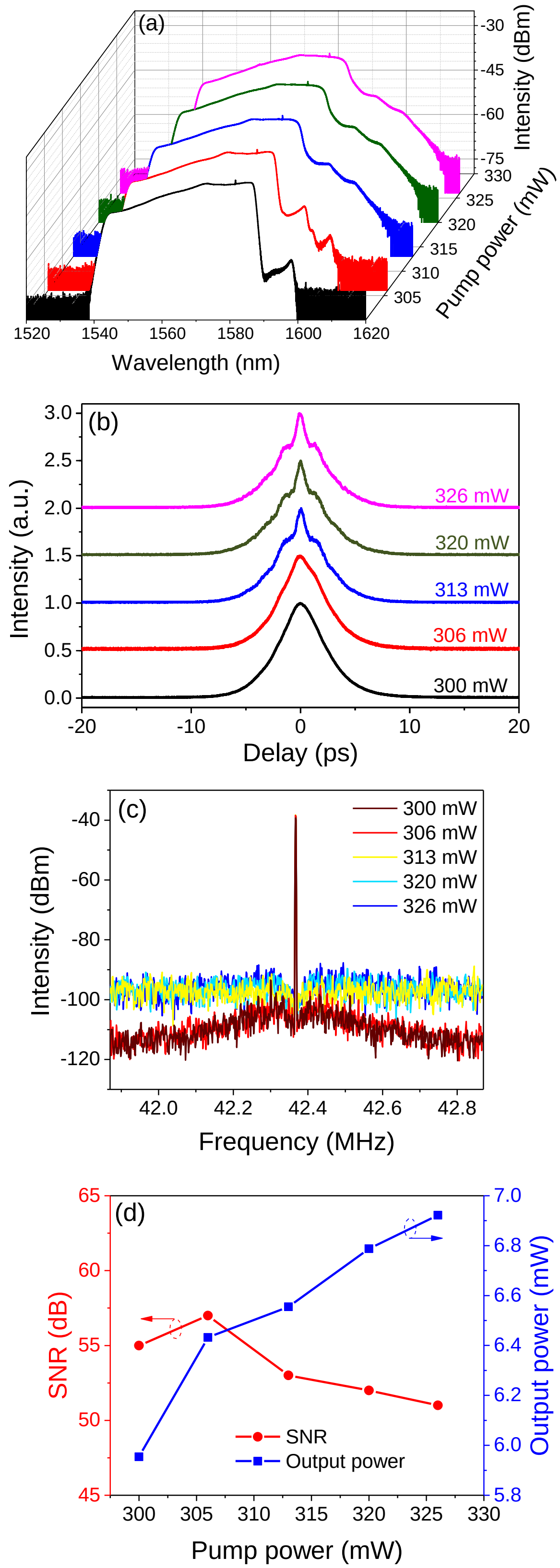

Fig. 5. Output pulses evolution features at different pump power levels, (a) optical spectra, (b) AC traces, (c) RF spectra, and (d) SNR (circle) and output power (box) versus pump power.

which implies that the transition of output pulse types in our laser is precisely and solely controlled by the pump power. The necessity of NLP is eliminated. Nonetheless, in other pulse states switchable lasers, it is usually necessary to fine adjust the PCs to achieve the switching conditions after changing pump power, which may cause the mode-locked state to be lost or unstable. This situation can be avoided when we use precise control of pump power instead, which implies our fiber laser possesses higher switching efficiency. The output pulses evolution features at different pump power levels are summarized in Fig. 5. The spectra have steep edges at pump power of 300 mW and 306 mW, which is a distinctive feature of DS. When the pump power is increased to 313 mW, the spectral sharp edges disappear and smoother spectrum is obtained, which is depicted in Fig. 5(a). At the same time, we can observe the evolution of AC traces in Fig. 5(b). As the pump power increases, the measured AC traces switch from Gaussian profiles to the double-scale structures. The evolution of the spectra and AC traces prove the output pulse types transformation from DS to NLP with the increasing of pump power [14]. This switching phenomenon is most likely attributed to the peak power clamping effect [14]. While the peak power of the DS reaches the CSP, further increasing pump power will break the DS into multiple pulses and then lead to the formation of the NLP [14,16,25]. The evolution of RF spectra under different pump power are illustrated in Fig. 5(c). When the output pulse types switch from DSs to NLPs, the pedestal of the RF spectrum will be lifted, which means the background noise of the NLPs is stronger than that of DSs. The SNR and output power versus the pump power are depicted in Fig. 5(d). When the fiber laser operates in the DS regime, the value of SNR increases with the pump power, but it is the opposite in the NLP regime. In addition, the SNR of NLP is smaller than that of DS. The average output power increases monotonically with pump power in both regimes, and the slope efficiency of the DS regime is higher than that of the NLP regime.

5. CONCLUSIONS

In summary, we demonstrate the pump precisely controlled switchable generation of DSs and NLPs in a net normal dispersion passively mode-locked EDFL using a 45° TFG. The output pulses can be flexibly switched between DSs and NLPs by simply changing the pump power. Therefore, eliminating the necessity of PCs adjustment for transformation between DS and NLP can make our laser possess higher switching efficiency. The NPR mode-locked mechanism consisting of a 45° TFG and two PCs plays an important role in switching of these two pulse types. We observe that the DS is centered at 1577 nm with the 3 dB bandwidth of 20.4 nm, and the typical NLP is centered at 1574 nm with the 3 dB bandwidth of 25.2 nm. The demonstrated laser also manifests the shortest laser cavity for NLP generation to date. We believe our work can make a contribution for further study of more physical formation mechanisms of the NLPs in the future. The demonstrated versatile laser may also find applications in various fields.

Funding. National Natural Science Foundation of China (NSFC) (61605107,61505244); Young Eastern Scholar Program at Shanghai Institutions of Higher Learning (QD2015027); "Young 1000 Talent Plan" Program of China and The Open Fund of Key Laboratory of Opto-electronic Information Technology; Ministry of Education (Tianjin University, China) (2018KFKT009)

REFERENCES

1. D. H. Deng, L. Zhan, Z. C. Gu, Y. Gu, and Y. X. Xia, "55-fs pulse generation without wave-breaking from an all-fiber Erbium-doped ring laser," Opt. Express **17**, 4284-4288 (2009).
2. J. S. Peng, L. Zhan, T. Y. Chen, Z. C. Gu, K. Qian, S. Y. Luo, and Q. S. Shen, "All-fiber ultrashort similariton generation, amplification, and compression at telecommunication band," J. Opt. Soc. Am. B **29**, 2270-2274 (2012).
3. X. L. Liu, H. S. Wang, Z. J. Yan, Y. S. Wang, W. Zhao, W. Zhang, L. Zhang, Z. Yang, X. H. Hu, X. H. Li, D. Y. Shen, C. Li, and G. D. Chen, "All-fiber normal-dispersion single-polarization passively mode-locked laser based on a 45°-tilted fiber grating," Opt. Express **20**, 19000-19005 (2012).
4. K. Tamura, R. D. Doerr, H. A. Haus, and E. P. Ippen, "Soliton fiber ring laser stabilization and tuning with a broad intracavity filter," IEEE Photonics Technol. Lett. **6**, 697-699 (1994).
5. K. Tamura, E. P. Ippen, H. A. Haus, and L. E. Nelson, "77-fs pulse generation from a stretched-pulse mode-locked all-fiber ring laser," Opt. Lett. **18**, 1080-1082 (1993).
6. B. Oktem, C. Ülgüdür, and F. Ö. Ilday, "Soliton–similariton fibre laser," Nat. Photonics **4**, 307-311 (2010).
7. A. Cabasse, B. Ortaç, G. Martel, A. Hideur, and J. Limpert, "Dissipative solitons in a passively mode-locked Er-doped fiber with strong normal dispersion," Opt. Express **16**, 19322-19329 (2008).
8. C. Lecaplain, B. Ortaç, and A. Hideur, "High-energy femtosecond pulses from a dissipative soliton fiber laser," Opt. Lett. **34**, 3731-3733 (2009).
9. S. Lefrançois, K. Kieu, Y. J. Deng, J. D. Kafka, and F. W. Wise, "Scaling of dissipative soliton fiber lasers to megawatt peak powers by use of large-area photonic crystal fiber," Opt. Lett. **35**, 1569-1571 (2010).
10. D. S. Kharenko, V. A. Gonta, and S. A. Babin, "50 nJ 250 fs all-fibre Raman-free dissipative soliton oscillator," Laser Phys. Lett. **13**, 025107 (2016).
11. Z. Sun, A. G. Rozhin, F. Wang, T. Hasan, D. Popa, W. O'Neill, and A. C. Ferrari, "A compact, high power, ultrafast laser mode-locked by carbon nanotubes," Appl. Phys. Lett. **95**, 253102 (2009).
12. K. Kieu, W. H. Renninger, A. Chong, and F. W. Wise, "Sub-100 fs pulses at watt-level powers from a dissipative-soliton fiber laser," Opt. Lett. **34**, 593-595 (2009).
13. D. Y. Tang, L. M. Zhao, and B. Zhao, "Soliton collapse and bunched noise-like pulse generation in a passively mode-locked fiber ring laser," Opt. Express **13**, 2289-2294 (2005).
14. L. M. Zhao, D. Y. Tang, and J. Wu, "Noise-like pulse in a gain-guided soliton fiber laser," Opt. Express **15**, 2145-2150 (2007).
15. S. Smirnov, S. Kobtsev, S. Kukarin, and A. Ivanenko, "Three key regimes of single pulse generation per round trip of all-normal-dispersion fiber lasers mode-locked with nonlinear polarization rotation," Opt. Express **20**, 27447-27453 (2012).
16. X. L. Li, S. Zhang, M. Han, and J. Liu, "Fine-structure oscillations of noise-like pulses induced by amplitude modulation of nonlinear polarization rotation," Opt. Lett. **42**, 4203-4206 (2017).
17. M. Horowitz, Y. Barad, and Y. Silberberg, "Noiselike pulses with a broadband spectrum generated from an erbium-doped fiber laser", Opt. Lett. **22**, 799-801 (1997).
18. S. Keren, and M. Horowitz, "Interrogation of fiber gratings by use of low-coherence spectral interferometry of noiselike pulses," Opt. Lett. **26**, 328-330 (2001).
19. E. Hernández-Escobar, M. Bello-Jiménez, O. Pottiez, B. Ibarra-Escamilla, R. López-Estopier, M. Durán-Sánchez, E. A. Kuzin, and M. V. Andrés, "Flat supercontinuum generation pumped by amplified noise-like pulses from a figure-eight erbium-doped fiber laser," Laser Phys. Lett. **14**, 105104 (2017).
20. A. Zaytsev, C. H. Lin, Y. J. You, C. C. Chung, C. L. Wang, and C. L .Pan, "Supercontinuum generation by noise-like pulses transmitted through normally dispersive standard single-mode fibers," Opt. Express **21**, 16056-16062 (2013).
21. Y. J. You, C. M. Wang, Y. L. Lin, A. Zaytsev, P. Xue, and C. L. Pan, "Ultrahigh-resolution optical coherence tomography at 1.3μm central wavelength by using a supercontinuum source pumped by noise-like pulses," Laser Phys. Lett. **13**, 025101 (2016).
22. G. Sobon, J. Sotor, T. Martynkien, and K. M.Abramski, "Ultra-broadband dissipative soliton and noise-like pulse generation from a normal

dispersion mode-locked Tm-doped all-fiber laser," Opt. Express **24**, 6156-6161 (2016).
23. J. H. Lin, C. L. Chen, C. W. Chan, W. C. Chang, and Y. H. Chen, "Investigation of noise-like pulses from a net normal Yb-doped fiber laser based on a nonlinear polarization rotation mechanism," Opt. Lett. **41**, 5310-5313 (2016).
24. H. D. Xia, H. P. Li, G. L. Deng, J. F. Li, S. J. Zhang, and Y. Liu, "Compact noise-like pulse fiber laser and its application for supercontinuum generation in highly nonlinear fiber," Appl. Opt. **54**, 9379-9384 (2015).
25. Y. Jeong, L. A. Vazquez-Zuniga, S. Lee, and Y. Kwon, "On the formation of noise-like pulses in fiber ring cavity configurations," Opt. Fiber Technol. **20**, 575-592 (2014).
26. Q. Q. Wang, T. Chen, M. S. Li, B. T. Zhang, Y. F. Lu, and K. P. Chen, "All-fiber ultrafast thulium-doped fiber ring laser with dissipative soliton and noise-like output in normal dispersion by single-wall carbon nanotubes," Appl. Phys. Lett. ***103***, 011103 (2013).
27. S. Kobtsev, S. Smirnov, and S. Kukarin, "Double-scale pulses generated by mode-locked fibre lasers and their applications," Fiber Laser ed M Paul (InTech) pp 69–88 (2016).
28. Z. S. Deng, G. K. Zhao, J. Q. Yuan, J. P. Lin, H. J. Chen, H. Z. Liu, A. P. Luo, H. Cui, Z. C. Luo, and W. C. Xu, "Switchable generation of rectangular noise-like pulse and dissipative soliton resonance in a fiber laser," Opt. Lett. **42**, 4517-4520 (2017).
29. Z. J. Yan, C. B. Mou, K. M. Zhou, X. F. Chen, and L. Zhang, "UV-Inscription, polarization-dependant loss characteristics and applications of 45° tilted fiber gratings," J. Lightwave Technol. **29**, 2715-2724 (2011).
30. K. M. Zhou, G. Simpson, X. F. Chen, L. Zhang, and I. Bennion, "High extinction ratio in-fiber polarizers based on 45° tilted fiber Bragg gratings," Opt. Lett. **30**, 1285-1287 (2005).
31. C. B. Mou, K. M. Zhou, L. Zhang, and I. Bennion, "Characterization of 45°-tilted fiber grating and its polarization function in fiber ring laser," J. Opt. Soc. Am. B **26**, 1905-1911 (2009).
32. C. B. Mou, H. Wang, B. G. Bale, K. M. Zhou, L. Zhang, and I. Bennion, "All-fiber passively mode-locked femtosecond laser using a 45°-tilted fiber grating polarization element," Opt. Express **18**, 18906-18911 (2010).
33. W. S. Man, H. Y. Tam, M. S. Demokan, P. K. A. Wai, and D. Y. Tang, "Mechanism of intrinsic wavelength tuning and sideband asymmetry in a passively mode-locked soliton fiber ring laser," J. Opt. Soc. Am. B **17**, 28-33 (2000).
34. L. M. Zhao, D. Y. Tang, X. Wu, and H, Zhang, "Dissipative soliton generation in Yb-fiber laser with an invisible intracavity bandpass filter," Opt. Lett. **35**, 2756-2758 (2010).
35. J. S. Peng, L. Zhan, Z. H. Gu, J. M. Liu, S. Y. Luo, X. H. Shen, and Q. S. Shen, "Modulation instability in dissipative soliton fiber lasers and its application on cavity net dispersion measurement," J. Lightwave Technol. **30**, 2707-2712 (2012).
36. C. B. Mou, R. Suo, K. M. Zhou, L. Zhang, and I. Bennion, "2nd order Bragg rasonance generated in a 45º tilted fiber grating and its application in a fiber laser," Bragg Gratings, Photosensitivity, & Poling in Glass Waveguides 2010 (Optical Society of America, 2010) BTuA7.
37. L. M. Zhao, and D. Y. Tang, "Generation of 15-nJ bunched noise-like pulses with 93-nm bandwidth in an erbium-doped fiber ring laser," Appl. Phys. B **83**, 553-557 (2006).
38. H. T. Zhang, G. Gao, Q. H. Li, and M. Gong, "High power double-scale pulses from a gain-guided double-clad fiber laser," Laser Phys. Lett. **14**, 035101 (2017).
39. P. Wang, D. K. Hu, K. J. Zhao, L. Y. Jiao, X. S. Xiao, and C. X. Yang, "Dissipative Rogue Waves Among Noise-Like Pulses in a Tm Fiber Laser Mode Locked by a Monolayer MoS2 Saturable Absorber," IEEE J. Sel. Top. Quantum Electron. **24**, 1800207 (2018).